Plane wave based method: Analytic integration and frequency behaviour

SOUFIEN ESSAHBI
Mechanical, Modelling and Manufacturing Unit (U2MP)
National Engineering School of Sfax (ENIS)
SFAX, Tunisia

EMMANUEL PERREY-DEBAIN
ROBERVAL laboratory
University of Technology of Compiègne
Street Roger Couttolenc, - BP 60319 - 60203 COMPIEGNE Cedex – France

MABROUK BEN TAHAR
ROBERVAL laboratory
University of Technology of Compiègne
Street Roger Couttolenc, - BP 60319 - 60203 COMPIEGNE Cedex – France

LOTFI HAMMAMI
Mechanical, Modelling and Manufacturing Unit (U2MP)
National Engineering School of Sfax (ENIS)
SFAX, Tunisia

MOHAMED HADDAR
Mechanical, Modelling and Manufacturing Unit (U2MP)
National Engineering School of Sfax (ENIS)
SFAX, Tunisia

soufien.essahbi@hotmail.fr

Abstract: - This paper deals with 2D acoustic problem. In order to study this problem, a finite element enriched by a plane wave base is used. This work focus on two aspects. Firstly, the study of this element depending on the frequency. Secondly, the description of an analytic integration technique. Two examples are studied, the first resemble to car cavity and the second resemble to rectangular duct. A comparison between numerical results obtained by standard finite element and enriched finite element are done, for the first one. And, for the second example, a comparison between numerical results obtained by the use of enriched finite element and analytic results are presented. With this work, the results found show that the performance of the enriched finite element increases while increasing the frequency, in the same way for the analytic integration.

Key-Words: - Helmholtz equation; Finite elements; Plane wave basis; Frequency behaviour; Analytic integration; GAUSS integration.

1 Introduction

Exposure to noise was a major environmental problem at the beginning of the 20th century and can be considered nowadays as a source of pollution. Controlling noise involves the implementation of two essential tools: noise prediction and noise reduction. Both of those tools are complimentary to establish an efficient control, either through reducing or absorbing noise. The need of cheap and efficient method to predict vibration is an urgent requirement.

Finite element method (FEM) [1] is still nowadays the most used to solve partial derivative equation systems resulting from modelling of physical problems, particularly in acoustic. Yet, the implementation of FEM and Boundary Element Method (BEM) [2] remains difficult and costly in certain cases, especially in medium and high frequencies. In fact, an accurate description of the

problem needs, sometime, 10 degrees of freedom (DOF) in the wave length [3], [4]. This great number of DOF can generates a complicate and hard solving problem. In order to overcome those difficulties, new methods appeared, for example, the PUFEM (Partition of Unity Finite Element Method) [5], [6] is used to solve Helmholtz equation [7], the generalized finite element method [8], which is a combination of the classical finite element method and the partition of unity method. According to this method, the functional space is built by multiplying classic form functions of finite elements by particular solutions for homogenous problems. Those particular solutions are oscillating functions (Trefftz approach) [9], [10].

Charbel developed the discontinuous enrichment method [11], [12], [13]. In this method the enrichment functions are calculated analytically. These functions are propagatory waves added to the bases functions of finite element. Ultra Weak Variational formulation (UWV) [14], [15] which consists in partitioning domains into sub domains with some adapted interface conditions is also used to solve the acoustics problems. The discretisation procedure of UWV is a physical approach which consists in approximating the solution by using plane waves. This formulation allows use of coarse mesh compared to frequency. Eventually, the wave based method [16]- [21] which is based on Trefftz methods is also used to treat those problems.

This paper is dedicated to the finite elements enriched by plane wave's method; a study depending on frequency will be presented later. The comparison between the numerical results obtained by simulation and the analytic expression results are presented in order to analyse the influence of the frequency increase on its finite enriched elements. The results show significant improvements in the number of used DOF. The second section of this paper deals with the development of the analytic integration technique; whish allows a considerable improvement in the calculation time.

2 Definition of the problem and variational formulation

Consider a 2D fluid cavity Ω (Fig.1), the border is subdivided into three parts Γ_p, Γ_v and Γ_Z. The cavity is filled by a fluid of density ρ_0.

The boundary conditions that have been taken are:

- And imposed pressure on Γ_p,
- Normal speed is set on the frontier Γ_v,
- Normal impedance on Γ_Z.

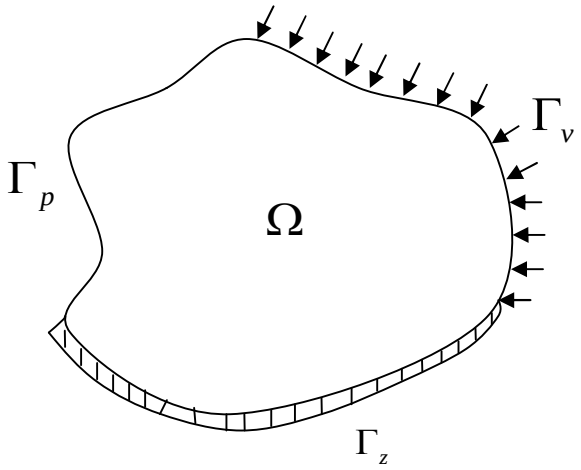

Fig.1 A 2D acoustic cavity.

The studied 2D problem is governed by Helmholtz equation and the boundary conditions given by the following equations:

Helmholtz equation:

$$\Delta p + k^2 p = 0 \tag{1}$$

With $\Delta = \frac{\partial^2}{\partial x^2} + \frac{\partial^2}{\partial y^2}$ represents the Laplace operator and k is the wave number given by:

$$k = \frac{\omega}{c}$$

Boundary conditions:

- *Dirichlet condition*

$$p(r) = \overline{p}(r); r \in \Gamma_p \tag{2}$$

- *Neumann condition*

$$\frac{\partial p(r)}{\partial n} = \rho_0 \omega \overline{v}_n(r);\ r \in \Gamma_v \tag{3}$$

- *Mixed condition*

$$\frac{\partial p(r)}{\partial n} = \rho_0 \omega \frac{p(r)}{\overline{Z}(r)};\ r \in \Gamma_z \tag{4}$$

with $\frac{\partial}{\partial n}$ the normal derivative and $\overline{p}(r)$, $\overline{v}_n(r)$ and $\overline{Z}(r)$ the prescribed values of the acoustic pressure, normal velocity and normal impedance.

Consider the Boundary Value Problem (BVP) described by (1) - (4), the first equation is multiplied

by a weighting function $p*$ which is supposed to be regular and integrated on Ω, so the result is represented by the equation (5):

$$\int_{\Omega} \Delta p(r)\, p*(r)\, d\Omega + k^2 \int_{\Omega} p(r)\, p*(r)\, d\Omega = 0 \quad (5)$$

By using the Green formula the former equation becomes:

$$\int_{\Omega} \nabla p(r) \nabla p*(r) d\Omega - k^2 \int_{\Omega} p(r)\, p*(r)\, d\Omega + \int_{\Gamma_v} \frac{\partial p(r)}{\partial n}\, p*(r)\, d\Omega_v \quad (6)$$

$$+ \int_{\Gamma z} \frac{\partial p(r)}{\partial n}\, p*(r)\, d\Omega_z = 0$$

Finally, the problem (6) is called the weak formulation of the BVP.

3 Plane Wave Based Method (PWBM)

The use of the FEM is generally accepted for dynamic response analyses. However, the FEM is practically limited to the low frequency range due to its computational costs, since the computational costs increase for increasing frequency. To provide a solution for problems in the mid-frequency range many methods are developped, like the Plane Wave Based Method (PWBM).

The aim of the PWBM is to enrich the bases functions of the standard finite element with plane waves which satisfy the Helmholtz homogeneous equation.

Fig.2. shows the linear triangular finite element geometry enriched by a plane wave basis which directions are 'attached' to the nodes.

The pressure is written for the standard finite element, under the sum of nodal values. This pressure is interpolated by the standard shape functions of the finite element given according to the local coordinates.

$$\begin{cases} N^1 = 1 - \xi - \eta \\ N^2 = \xi \\ N^3 = \eta \end{cases} \quad (7)$$

The nodes values are now approximated in the form of discrete plane waves propagating sum in different plan directions.

$$p = \sum_{h=1}^{Nne} p_h N^h(\xi, \eta) \quad (8)$$

With:

Nne : The number of nodes per element.

Where the pressure p_h is written in the form:

$$p_h = \sum_{q=1}^{N\_P\_W} \exp\left(ik\boldsymbol{\chi}_h^q . \boldsymbol{R}\right) p_h^q \quad (9)$$

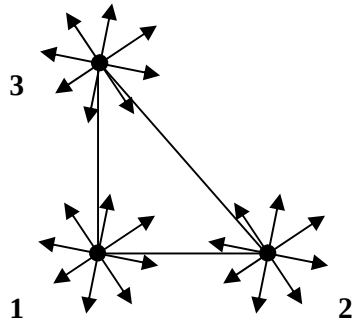

Fig.2 Enriched linear triangular finite element.

With:

- N_P_W : The number of directions of plane waves,
- p_h^q : The amplitudes of the plane waves.

The plane waves directions attached to each node are given by:

$$\boldsymbol{\chi}_h^q = \left(\cos\left(\frac{2\pi q}{N\_P\_W} \right), \sin\left(\frac{2\pi q}{N\_P\_W} \right) \right) \quad (10)$$

The vector R is the position vector of the calculating point on the meshing given by:

$$R = \left(\sum_{i=1}^{Nne} N^i(\xi,\eta)\, x_i, \sum_{i=1}^{Nne} N^i(\xi,\eta)\, y_i \right) = \left(\left\langle N^i(\xi,\eta) \right\rangle \{x_i\}, \left\langle N^i(\xi,\eta) \right\rangle \{y_i\} \right) \quad (11)$$

The shape functions of the finite enriched element are the interpolation functions of the standard finite element combined with the directions of plane waves. That implies for each node a N_P_W degrees of freedom instead of 1. The unknown quantities become the plane waves amplitude instead of being the node pressure values.

$$p = \sum_{h=1}^{Nne} N^h(\xi,\eta) \sum_{q=1}^{N\_P\_W} \exp\left(ik\boldsymbol{\chi}_h^q . \boldsymbol{R}\right) p_h^q \quad (12)$$

The shape functions for the triangular linear element in Figure 2 are described by the following equation:

$$R = \left(\sum_{i=1}^{Nne} N^i(\xi,\eta)\, x_i, \sum_{i=1}^{Nne} N^i(\xi,\eta)\, y_i \right) = \left(\left\langle N^i(\xi,\eta) \right\rangle \{x_i\}, \left\langle N^i(\xi,\eta) \right\rangle \{y_i\} \right) \quad (13)$$

The weighting function selected is the shape function conjugate.

$$p* = conj(p) \quad (14)$$

$conj\{\ \}$: is the conjugated function.

4 Numerical results

In this section the enriched finite elements and the standard finite elements are compared, by studying the enriched finite elements according to frequency. Then an analytic integration technique, used, is developed.

Firstly, a comparison between numerical results obtained by standard finite element and enriched finite element are presented. Then, a comparison between the numerical results obtained by simulation and the results of analytic expression are presented too.

The error percentage according to the number of *DOF* by wave length τ is calculated. The number of *DOF* by wave length τ is given by:

$$\tau = \lambda \times \sqrt{\frac{N\_Node \times N\_P\_W}{S}} \tag{15}$$

Where:

- N_Node : The mesh nodes number,
- S : The surface of the domain of study
- λ : The wave length presented by :

$$\lambda = \frac{2\pi}{k} \tag{16}$$

All exemples are treated with the analytical integration.

4.1 2D car-like cavity

Consider the 2D car cavity, shown in Fig.3, this bounded cavity is filled with air ($c_0 = 340\ m/s$, $\rho_0 = 1.225\ kg/m^3$) and excited by a normal acceleration boundary condition $\gamma_n = 1 m/s^2$ along the left vertical wall. Furthermore, the upper panels of the cavity, representing the roof of the car, are modelled as an acoustic normal impedance $\overline{Z}_n = (441 - 1241j)\ Pa.s/m$.

The impedance boundary condition represents the acoustic damping due to the trim components inside the car cavity.

The cavity dimensions are shown in Figure 3.

The considered problem represents a typical uncoupled acoustic problem, as it is frequently encountered in industry. The pressure field inside a closed cavity needs to be determined, given an acceleration and damping distribution on the cavity boundary. Typically, an analysis engineer is interested in predicting the pressure field up to a few *kHz*.

This example is treated using the standard triangular linear finite elements and the finite enriched triangular linear elements. The following Fig.4 and 5 illustrate the meshes used in the two studies.

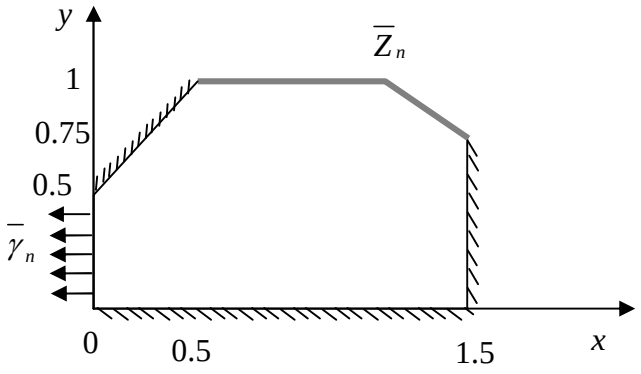

Fig.3 A 2D car-like cavity.

The standard triangular finite element mesh includes 55830 nodes and 111658 elements.

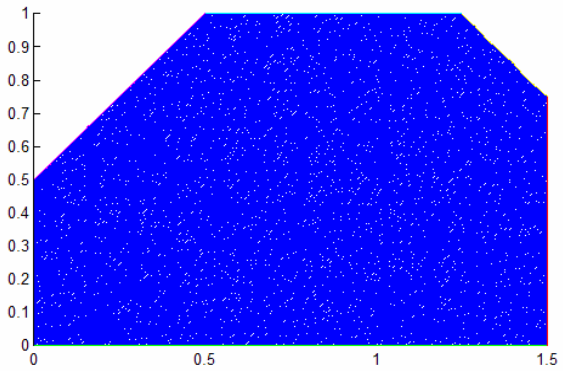

Fig.4 A standard finite element mesh.

In the Fig.5 the enriched triangular finite element mesh includes 37 nodes and 72 elements.

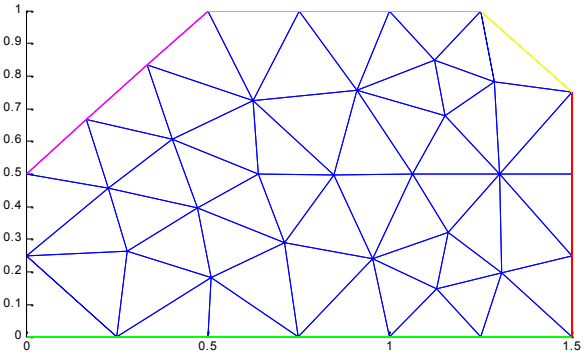

Fig.5 An enriched finite element mesh.

The Fig.6 and 7 show the fluid cavity pressure (for a wave number equal to 20).

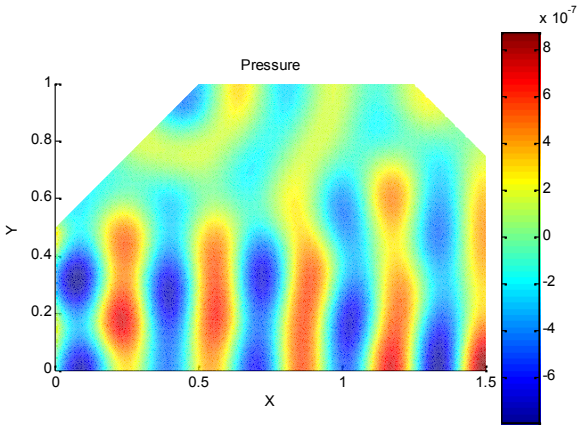

Fig.6 Pressure amplitude contour plot at k = 20 calculated with the FEM.

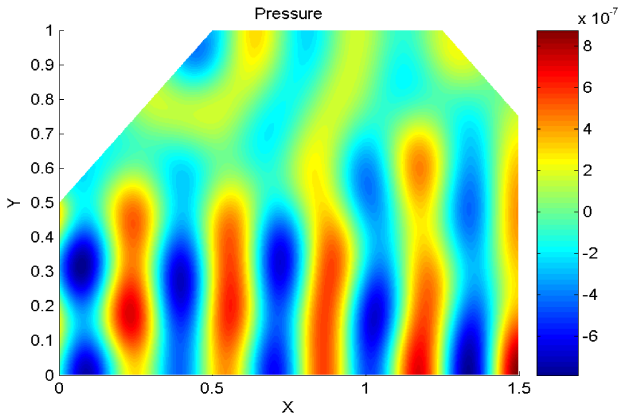

Fig.7 Pressure amplitude contour plot at k = 20 calculated with the *PWBM*.

The Table 1 illustrate the comparison between the standard finite elements and the enriched finite elements.

Table 1. Comparison between standard finite elements and the enriched finite elements.

	Standard finite element	Enriched finite element
Node number	55830 nodes	37 nodes
Element number	111658elements	72 elements
Degree of freedom	55830 *DOF*	370 *DOF*
Time	624,484 (s) (10 mn 24 s)	2,187 (s)

According to this Table, the enriched elements allows space memory gain, it need only 370 *DOF* instead of 55830 *DOF*. These elements reduce the time calculation from 624,484(s) to 2,187(s).

4.2 Wave propagation in a duct with rigid walls

This paragraph deals with the distribution of pressure in the space limited by a rectangular duct. Acceleration is imposed to one of the duct sides, impedance on other and the remained sides are rigid. This pressure distribution, determined by using enriched linear triangular finite element, is compared to an analytic solution.

Fig.8 represents the rectangular duct study domain.

The problem is defined by:

$$\begin{cases} \Delta p + k^2 p = 0 & x \in \Omega \quad (a) \\ \dfrac{\partial p}{\partial n} = \cos(m\pi y) & at\ x = 0 \quad (b) \\ \dfrac{\partial p}{\partial n} + ikp = 0 & at\ x = 2 \quad (c) \\ \dfrac{\partial p}{\partial n} = 0 & at\ y = 0,1 \quad (d) \end{cases} \tag{17}$$

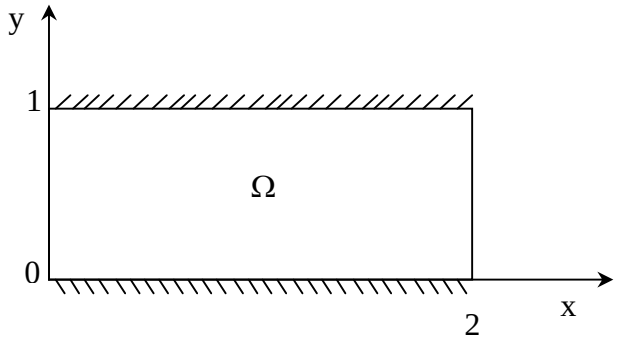

Fig.8 Rectangular duct.

The inlet boundary x = 0 has an inhomogeneous Neumann condition and the outlet boundary x = 2 is characterized using an absorbing boundary condition. The boundaries y = 0;1 are assumed perfectly rigid leading to vanishing normal derivatives on the boundary.

4.2.1 Analytical resolution

The pressure can be written as follows:

$$p(x,y) = X(x)Y(y) \tag{18}$$

Taking the boundary conditions x = 0, (17. b) becomes:

$$\frac{\partial p(0,y)}{\partial n} = \cos(m\pi y) = -\frac{dX(0)}{dx}Y(y) \tag{19}$$

This equation is equivalent to the following equations system:

$$\begin{cases} Y(y) = -\cos(m\pi y) \\ \dfrac{dX(0)}{dx} = 1 \end{cases} \tag{20}$$

Hence the pressure can be written as follows:

$$p(x,y) = -X(x)\cos(m\pi y) \quad (21)$$

Injecting this expression into the Helmholtz equation we obtain:

$$\left(\frac{d^2X(x)}{dx^2} + (m\pi)^2 X(x) - k^2 X(x)\right)\cos(m\pi y) = 0\ ;\ \forall y \quad (22)$$

$$\Rightarrow \frac{d^2X(x)}{dx^2} - \left(k^2 - (m\pi)^2\right)X(x) = 0 \quad (23)$$

It is a second degree differential equation without second member.

So the component along the direction of the pressure is written:

$$X(x) = A_1 e^{ik_x x} + A_2 e^{-ik_x x} \quad (24)$$

with

$$\sqrt{k^2 - (m\pi)^2} = k_x \quad (25)$$

The analytic expression of the pressure in the duct is presented by the following equation:

$$p(x,y) = \cos(m\pi y)\left(A_1 e^{-ik_x x} + A_2 e^{ik_x x}\right) \quad (26)$$

With:

$$k_x = \sqrt{\left(k^2 - (m\pi)^2\right)} \quad (27)$$

Hence the sound pressure is given by:

$$p(x,y) = -\left(A_1 e^{ik_x x} + A_2 e^{-ik_x x}\right)\cos(m\pi y) \quad (28)$$

To determine the constant A_1 and A_2 the pressure expression (26) is substituted in the mixed boundary condition equation (17. c) and the derivative of $X(x)$ is taken along the x direction.

Finally, A_1 and A_2 coefficients satisfy the equation:

$$i\begin{pmatrix} k_x & -k_x \\ (k+k_x)e^{2ik_x} & (k-k_x)e^{-2ik_x} \end{pmatrix}\begin{pmatrix} A_1 \\ A_2 \end{pmatrix} = \begin{pmatrix} 1 \\ 0 \end{pmatrix} \quad (29)$$

4.2.2 Analytical-numerical comparison

The solution represents propagating modes when the mode number m is below the cut-off value $m_{cut-off}$.

$$m \le m_{cut-off} = \frac{k}{\pi} \quad (30)$$

The modes for which $m \succ m_{cut-off}$ are evanescent. To measure the accuracy of the numeric solution to that analytic one, error L_2 should be introduced as follows:

$$Error(\%) = 100\frac{\left\|p_{ex} - p_{app}\right\|_{L_2(\Omega)}}{\left\|p_{ex}\right\|_{L_2(\Omega)}} \quad (31)$$

With:

p_{ex} : Exact pressure (analytic),

p_{app} : Approximate pressure numerically calculated,

$\|\ \|_{L_2}$: Norm 2.

The simulations are performed for the wave numbers k = 20; 40 and 80 when the corresponding to propagating mode number m = 6 and the first evanescing mode number.

The mesh used in the simulation is shown in Fig.9. This mesh consists of 22 finite elements insides the domain and 12 finite elements on the boundaries.

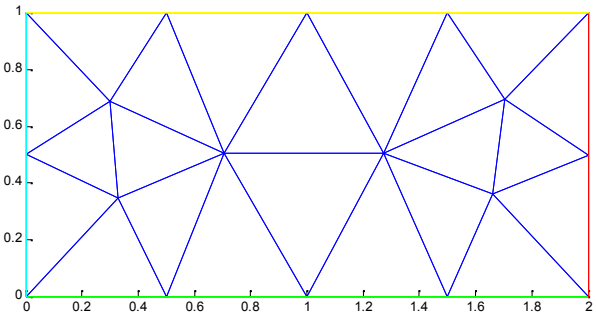

Fig.9 Triangular enriched finite element mesh.

Subsequently, the pressure distribution in the domain of study is determined for the 6th mode, for different frequencies f = 1082, 2164.5 and 4329 *Hz*.

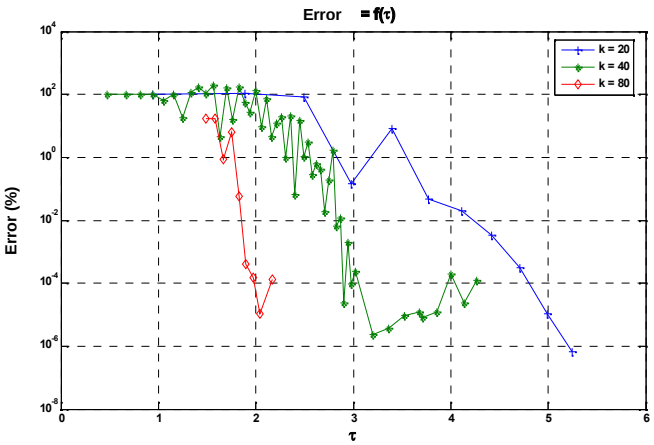

Fig.10 Error according to τ for $m = 6$ and k = 20; 40 and 80
(Linear enriched triangular element).

In conclusion, according to this figure, in order to insure satisfactory error between 10^{-1} and 10^{-7}, it would be enough to use:

- 3.2 to 5 degrees of freedom by wave length for the frequency f = 1082 *Hz*,
- 2 to 3 degrees of freedom by wave length for the frequency f = 2164.5 *Hz*,
- 1.8 to 2 degrees of freedom by wave length for the frequency f = 4329 *Hz*.

Which is not the case when using standard finite elements, that needs about 10 degrees of freedom by wave length [3] to have the same error order.

It is also possible to conclude that the number of *DOF* by wave length necessary to obtain the same error decrease when increasing the frequency. These results show that the enriched finite element by plane wave basis performance increases while increasing the frequency. To have a idea about the pressure distribution in the duct for its different frequencies, the Fig.11 shows the pressure topography for the 6th mode and the Fig.12, the first non propagative mode.

4.3 Integration technique

In the former studies, integration of the exponential functions was evaluated by using high scale integration, for example, Gauss Legendre integration [22]. In fact, the exponential terms generate a great oscillation in the finite elements.

For example, in the case of a plane wave diffracted by a rigid cylinder O. Lagrouche and P. Bettes [22] used more than 120 by 120 points of Gauss to evaluate the integrals ($ka = 10\pi$).

In this part the analytic technique integration is developed. Then a comparison between the results found by using this technique and Gauss point integration technique will be presented.

The problem consists on the wave function integration on the triangle surface (the polynomial function by an exponential complex function product) this integral is defined by:

$$
\begin{aligned}
I = I^{lj} &= \iint_{Tréf} N^l N^j e^{\left(-iK\chi_q.R\right)} e^{\left(iK\chi_m.R\right)} J\, d\xi d\eta \\
&= \iint_{Tréf} N^l N^j e^{(i(\alpha\xi+\beta\eta+\gamma))} J\, d\xi d\eta \\
&= \begin{cases}
\iint_{Tréf} (1-\xi-\eta)^2 e^{(i(\alpha\xi+\beta\eta+\gamma))} J\, d\xi d\eta, \\
\iint_{Tréf} (1-\xi-\eta)\xi e^{(i(\alpha\xi+\beta\eta+\gamma))} J\, d\xi d\eta, \\
\iint_{Tréf} (1-\xi-\eta)\eta e^{(i(\alpha\xi+\beta\eta+\gamma))} J\, d\xi d\eta, \\
\iint_{Tréf} \xi^2 e^{(i(\alpha\xi+\beta\eta+\gamma))} J\, d\xi d\eta, \\
\iint_{Tréf} \xi\eta e^{(i(\alpha\xi+\beta\eta+\gamma))} J\, d\xi d\eta, \\
\iint_{Tréf} \eta^2 e^{(i(\alpha\xi+\beta\eta+\gamma))} J\, d\xi d\eta
\end{cases}
\end{aligned}
\tag{32}
$$

Where:

N^l, N^j : Shape functions of standard finite elements,

$\boldsymbol{R}(x, y)$: Vector position,

$\boldsymbol{\chi}$: Vector characterizing the calculation point coordinates,

α, β and γ Constants according to calculation point coordinates,

J : The Jacobien matrix determinant,

T_{ref} : Reference triangle.

To calculate this integral, it would be enough to calculate the integral W below. The integral I can be written in a linear combination form of the integral W and its derivatives regarding to α and β.

$$
W = \iint_{Tréf} e^{(i(\alpha\xi+\beta\eta))} d\xi d\eta = \frac{\alpha e^{i\beta} - \beta e^{i\alpha} - \alpha + \beta}{\alpha\beta(\alpha-\beta)} \tag{33}
$$

It is obvious that there exist some singularity when α, β or $(\alpha-\beta)$ tend to zero. For that reason four calculation zones will be defined as follows:

$$
\begin{aligned}
&\alpha \in \vartheta(0) \,\&\, \beta \notin \vartheta(0) \\
&\alpha \notin \vartheta(0) \,\&\, \beta \in \vartheta(0) \\
&\alpha \in \vartheta(0) \,\&\, \beta \in \vartheta(0) \\
&(\alpha-\beta) \in \vartheta(0) \,\&\, \alpha \notin \vartheta(0) \,\&\, \beta \notin \vartheta(0)
\end{aligned}
\tag{34}
$$

Where $\vartheta(0)$ near zero.

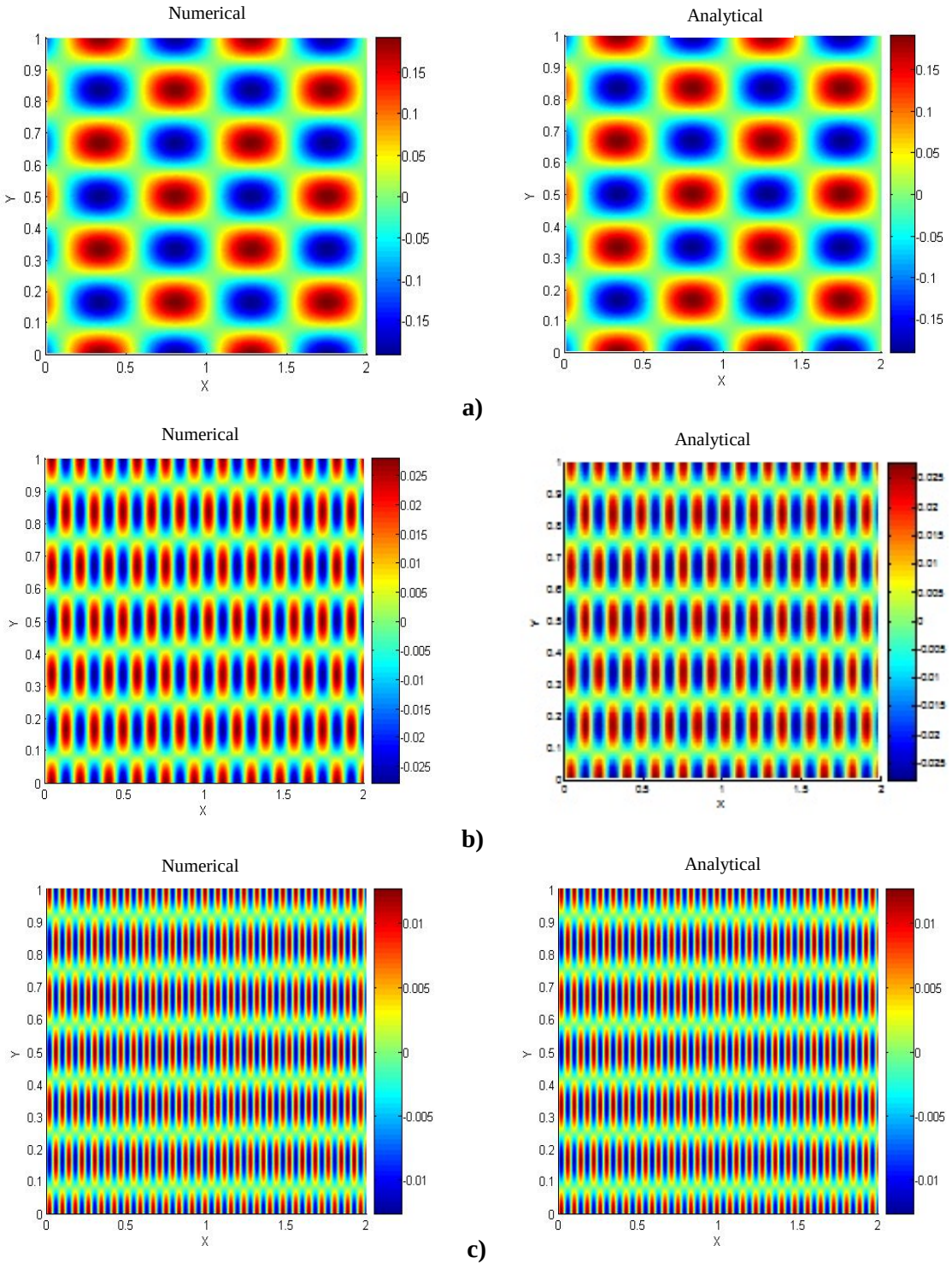

Fig. 1. Analytical and numerical pressure distribution for the 6th mode

a) $k = 20$; *b)* $k = 40$; *c)* $k = 80$

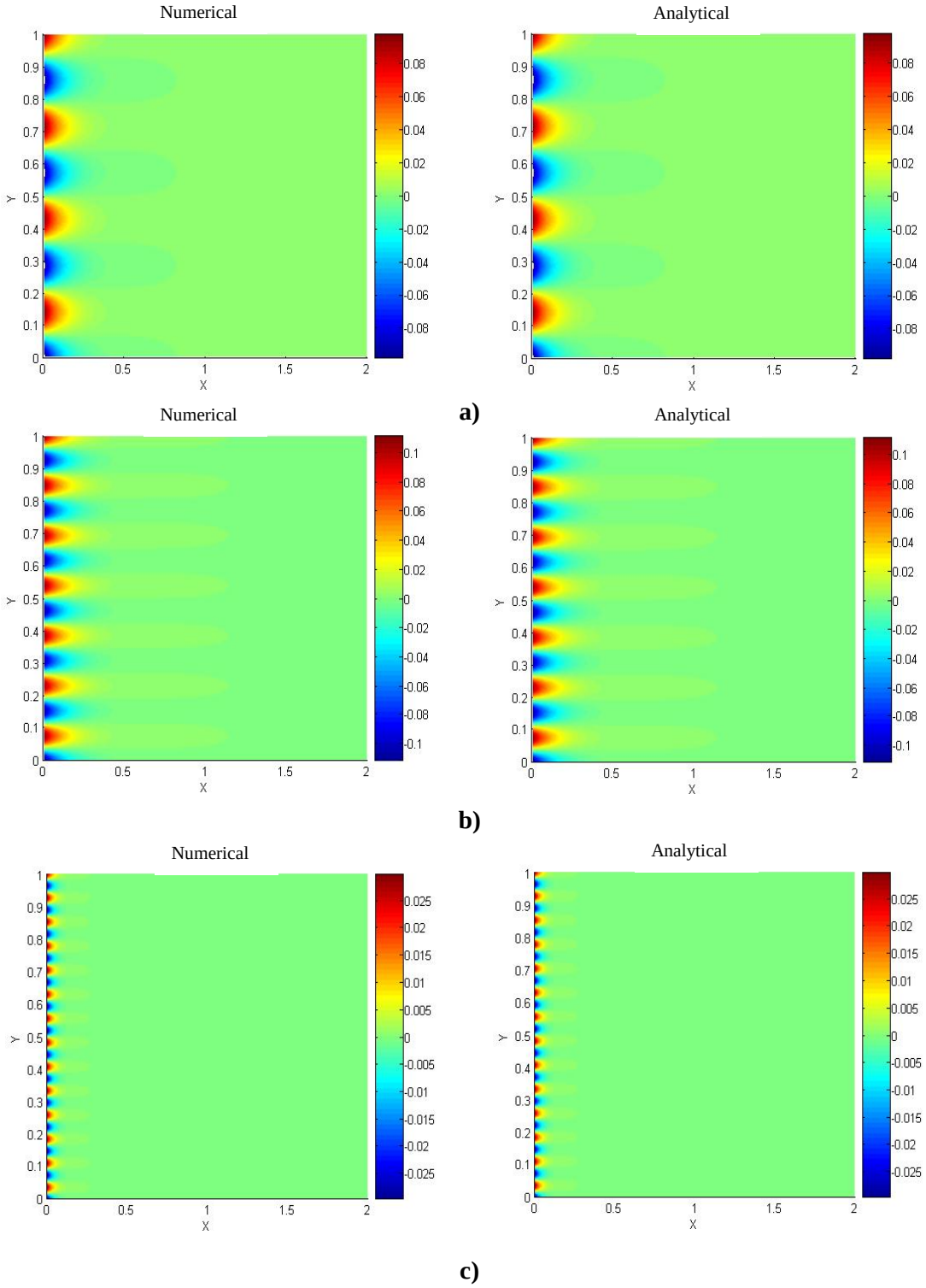

Fig. 2. Analytical and numerical pressure distribution for the first evanescing mode

a) $k = 20$; *b)* $k = 40$; *c)* $k = 80$

Beyond these zones, this integral calculation is normally done with a primitive formula.

Fig.13 shows the different calculation zones.

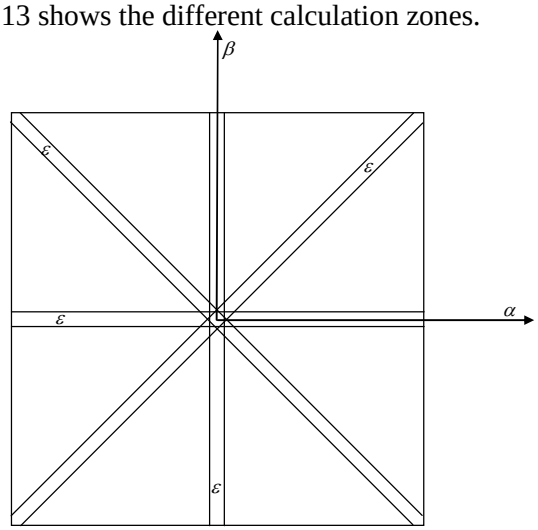

Fig.13 Different calculation zones.

In the first three zones the limited development close to zero of the functions $\{e^{i\alpha}\}$, $\{e^{i\beta}\}$ and $\{e^{i\alpha}, e^{i\beta}\}$ is done respectively. Not simplified form fourth zone for W is taken as follow:

$$W = -\frac{e^{i\alpha}}{\alpha}\frac{e^{i(\beta-\alpha)}-1}{(\beta-\alpha)} + \frac{1}{\alpha}\frac{e^{i\beta}-1}{\beta} \tag{35}$$

$W_1 = \dfrac{e^{i(\beta-\alpha)}-1}{(\beta-\alpha)}$ represents a singularity for $(\beta-\alpha) \in \vartheta(0)$, so the limited development of the function is done close to zero.

The integrals I^{lj} are written according to W and its derivatives as follows:

$$\begin{aligned}
I^{11} &= Je^{(i\gamma)}\left[W + 2i\frac{\partial W}{\partial\alpha} + 2i\frac{\partial W}{\partial\beta} - \frac{\partial^2 W}{\partial^2\alpha} - 2\frac{\partial^2 W}{\partial\alpha\partial\beta} - \frac{\partial^2 W}{\partial^2\beta}\right]\\
I^{12} &= Je^{j\gamma}\left[-i\frac{\partial W}{\partial\alpha} + \frac{\partial^2 W}{\partial^2\alpha} + \frac{\partial^2 W}{\partial\alpha\partial\beta}\right]\\
I^{13} &= Je^{j\gamma}\left[-i\frac{\partial W}{\partial\beta} + \frac{\partial^2 W}{\partial\alpha\partial\beta} + \frac{\partial^2 W}{\partial^2\beta}\right]\\
I^{22} &= -Je^{\gamma}\frac{\partial^2 W}{\partial^2\alpha}\\
I^{23} &= -Je^{\gamma}\frac{\partial^2 W}{\partial\alpha\partial\beta}\\
I^{33} &= -Je^{\gamma}\frac{\partial^2 W}{\partial^2\beta}
\end{aligned} \tag{36}$$

Either the θ and φ angles characterizing the two plane wave basis position vectors, these two angles are given by:

$$\begin{aligned}
\theta &= \frac{2\pi q}{N_P_W}\ ; \qquad 1 \le q \le N_P_W\\
\varphi &= \frac{2\pi n}{N_P_W}\ ; \qquad 1 \le n \le N_P_W
\end{aligned} \tag{37}$$

Where the χ_q and χ_n vectors are given by:

$$\begin{aligned}
\chi_q &= \left(\cos(\theta), \sin(\theta)\right)\\
\chi_n &= \left(\cos(\varphi), \sin(\varphi)\right)
\end{aligned} \tag{38}$$

The integral I can be written under the following shape:

$$I = \iint_{Tref} N^l N^j e^{\left(iK\left[(\cos(\varphi)-\cos(\theta))x + (\sin(\varphi)-\sin(\theta))y\right]\right)} J\, d\xi d\eta \tag{39}$$

By identification the α, β and γ constants are given by:

$$\begin{aligned}
\alpha &= k\left[(\cos(\theta)-\cos(\varphi))(x_1-x_2) + (\sin(\theta)-\sin(\varphi))(y_1-y_2)\right]\\
\beta &= k\left[(\cos(\theta)-\cos(\varphi))(x_1-x_3) + (\sin(\theta)-\sin(\varphi))(y_1-y_3)\right]\\
\gamma &= k\left[(\cos(\varphi)-\cos(\theta))x_1 + (\sin(\varphi)-\sin(\theta))y_1\right]
\end{aligned} \tag{40}$$

Where:

x_j, y_j : The coordinates of j node.

In order to test and to validate this integration technique a comparison between the calculation times for the two technical will be presented.

The error according to τ (evoked in subsection § 4.2.2) will be presented for the two integrations techniques for a wave number $k = 20, 40$ and 80.

While comparing the results given by the Figure 14, respecting acceptable error, the analytic integration needed time is less than the Gauss points integration time. The ratio calculation time between those tow techniques $\left(\frac{\text{time of the analytic integration}}{\text{time of the numeric integration}}\right)$ decreases while increasing the frequency, it represent the $\frac{1}{5}$th for a wave number $k = 20$ and it nearly reaches $\frac{1}{10}$ for a wave number $k = 80$.

4 Conclusion

This article describes the plane wave basis method. This paper aimed to the study of these enriched elements according to the frequency so the development of the, used, integration technique.

The validation examples clearly illustrate the potential of the PWBM to predict accurate results with substantially smaller prediction models compared with the FEM. The small model size of the PWBM, together with the high convergence rate, make it a less computationally demanding method than the FEM, which creates opportunities for the PWBM to tackle problems at higher frequencies, as compared to the low-frequency applicability of the FEM. The gotten results show the performance of the PWBM in the gain of the space memory and the time calculation. And these results show that, while increasing the frequency of excitation, the necessary number of DOF by wave length decreases.

The analytic technique integration is developed, exact expressions have been derived for the integrals of products of polynomials and exponentials functions. The results prove that the using analytic integration technique, the time of calculation decreases while increasing the frequency. We can reduce the time of calculation until $1/10$ of calculation time put by the GAUSS points integration technique for a wave number $k = 80$.

References

[1] O. Zienkiewicz, R. L. Taylor, *La méthode des éléments finis : formulation de base et problèmes linéaires*, trad. par Jacques-Hervé Saïac, Jérôme Jaffré, Michel Kern... [et al.] - [4e éd.] -Paris- La Défense : AFNOR, 1991 (Paris), Impr. Jouve .- XVIII-620 p : ill., couv. ill : 24 cm .- AFNOR technique .- ISBN 2-12-301111-8 (rel.).

[2] George C. Hsiao ,Boundary element methods—An overview, *Applied Numerical Mathematics* ,56 ,2006, pp. 1356–1369.

[3] E. Perrey-Debain, J. Trevelyan, P. Bettess, Wave boundary elements: a theoretical overview presenting applications in scattering of short waves, *Engineering Analysis with Boundary Elements*,28 , 2004, pp. 131–141.

[4] F. Ihlenburg, Finite Element Analysis of Acoustic Scattering,, *Springer- Verlag*, New York, 1998.

[5] J.M. Melenk & I. Babuska, The partition of unity finite element method: Basic theory and applications, *Comput. Methods Appl. Mech. Engrg.*, 139,1996, pp. 289-314.

[6] Babuska & J.M. Melenk, The partition of unity method, *International journal for numerical methods in engineering*, 40, 1997, pp.727-758.

[7] P. Ortiz & E. Sanchez , An improved partition of unity finite element model for diffraction problems, *Int. J. Numer. Meth. Engng.*, 50, 2001, pp. 2727-2740.

[8] R.J. Astley & P. Gamallo, Special short wave elements for flow acoustics, *Computer Methods in Applied Mechanics and Engineering*,194, 2005, pp. 341-353.

[9] B. Pluymers, W. Desmet, D. Vandepitte & P. Sas, Feasibility study of the wave based method for high-frequency steady-state acoustic analysis, *Proceedings of ISMA* , 2004, pp. 1555-1573.

[10] Z.C. Li, The Trefftz method for the Helmholtz equation with degeneracy, *Applied Numerical Mathematics*, 2008, 58, pp.131–159.

[11] Charbel Farhat, Isaac Harari, Leopoldo P. Franca, The discontinuous enrichment method, *Comput. Methods Appl. Mech. Engrg.* , 2001, 190, pp. 6455-6479.

[12] Charbel Farhat, Isaac Harari, Ulrich Hetmaniuk, A discontinuous Galerkin method with Lagrange multipliers for the solution of Helmholtz problems in the mid-frequency regime, *Comput. Methods Appl. Mech. Engrg.* , 2003, 192, pp. 1389-1419.

[13] Charbel Farhat, Paul Wiedemann-Goiran, Radek Tezaur, A discontinuous Galerkin method with plane waves and Lagrange multipliers for the solution of short wave exterior Helmholtz problems on unstructured meshes, *Wave Motion* , 2004, 39, pp. 307–317.

[14] Tomi Huttunen, Peter Monk, Jari P. Kaipio, Computational Aspects of the Ultra-Weak

Variational Formulation, *Journal of Computational Physics*, 2002, 182, pp.27– 46.

[15] T. Huttunen, P. Monk, F. Collino, and J.P. Kaipio, The ultra weak variational formulation for elastic wave problems, *SIAM Journal on Scientific Computing*, 2004, 25(5), pp.1717–1742.

[16] Wim Desmet, A wave based prediction technique for coupled vibro-acoustic analysis, 1998, Ph.D. thesis 98D12, Katholieke universiteit LEUVEN, Leuven, Belgium

[17] B. Van Hal, C. Vanmaele, Wim Desmet, P. Silar, H. –H. Priebsch, Hybrid finite element – Wave based method for steady – state acoustic analysis, *PROCEEDINGS OF ISMA,2004*, pp. 1629 – 1642.

[18] B. van Hal, W. Desmet , D. Vandepitte, Hybrid finite element—wave-based method for steady-state interior structural–acoustic problems, *Computers and Structures*, 2005, 83, pp. 167–180.

[19] B. Van Genechten, B. Pluymers, C. Vanmaele, D. Vandepitte, W. Desmet, On the coupling of wave based models with modally reduced finite element models for structural-acoustic analysis, *PROCEEDINGS OF ISMA*, 2006 , pp. 2383 – 2403.

[20] Bert Van Genechten, Bert Pluymers, Caroline Vanmaele Dirk Vandepitte, Wim Desmet, Application of modal model reduction for hybrid structural finite element – acoustic wave based models, *Proceedings of the Fourteenth International Congress on Sound and Vibration (ICSV14)*, 2007, Cairns, Australia

[21] Bert Pluymers, Dirk Vandepitte, Paul Sas, Wim Desmet, On the use of high-order finite element-wave based method for interior acoustic cavity analysis, *Proceedings of the Fourteenth International Congress on Sound and Vibration (ICSV14)*, 2007, Cairns, Australia

[22] O. Lagrouche & P. Bettess, short wave modelling using special finite elements, *Journal of Computational Acoustics*, 2000, 8(1), pp.189-210.